

New cross section measurements for neutron-induced reactions on Cr, Ni, Cu, Ta and W isotopes obtained with the activation technique

V. Semkova^{1,2}, R. Capote³, R. Jaime Tornin¹, A.J. Koning⁴, A. Moens¹, and A.J.M. Plompen¹

¹ European Commission, DG-Joint Research Centre, Institute for Reference Materials and Measurements, 2440 Geel, Belgium

² Institute for Nuclear Research and Nuclear Energy, 1784 Sofia, Bulgaria

³ International Atomic Energy Agency – Nuclear Data Section, P.P. Box 100, 1400 Vienna, Austria

⁴ Nuclear Research and Consultancy Group NRG, P.O. Box 25, 1755 ZG Petten, The Netherlands

Abstract. Herein we report on $^{50}\text{Cr}(n,x)^{48}\text{V}$, $^{58}\text{Ni}(n,p\alpha)^{54}\text{Mn}$, $^{58}\text{Ni}(n,x)^{56}\text{Co}$, $^{63}\text{Cu}(n,p\alpha)^{59}\text{Fe}$, $^{181}\text{Ta}(n,\alpha)^{178\text{m}}\text{Lu}$, $^{181}\text{Ta}(n,\alpha)^{178\text{g}}\text{Lu}$, $^{181}\text{Ta}(n,x)^{180\text{m}}\text{Hf}$, $^{181}\text{Ta}(n,p)^{181}\text{Hf}$, $^{181}\text{Ta}(n,2n)^{180\text{g}}\text{Ta}$, $^{182}\text{W}(n,p)^{182}\text{Ta}$, $^{183}\text{W}(n,x)^{182}\text{Ta}$, $^{183}\text{W}(n,p)^{183}\text{Ta}$, $^{184}\text{W}(n,x)^{183}\text{Ta}$, $^{184}\text{W}(n,\alpha)^{181}\text{Hf}$, $^{184}\text{W}(n,p)^{184}\text{Ta}$, $^{186}\text{W}(n,\alpha)^{183}\text{Hf}$, $^{186}\text{W}(n,x)^{185}\text{Ta}$, $^{186}\text{W}(n,p)^{186}\text{Ta}$, and $^{186}\text{W}(n,2n)^{185\text{m}}\text{W}$ reaction cross section measurements using the activation technique. The irradiations were carried out at the 7-MV Van de Graaff accelerator at IRMM, Geel. Quasi monoenergetic neutrons with energies between 13.8 and 20.5 MeV were produced via the $^3\text{H}(d,n)^4\text{He}$ reaction at $E_d = 1, 2, 3,$ and 4 MeV. Both natural and samples enriched in ^{182}W , ^{183}W , ^{184}W , and ^{186}W were used to facilitate correction for interference between reactions leading to the same product. Standard γ -ray spectrometry was employed for the measurement of the radioactivity. In addition to the standard detector efficiency calibration a Monte Carlo simulation of the coaxial HPGe detector was performed with the MCNP5 code in order to achieve higher geometry flexibility and better accuracy. The measured results are compared with work by other authors, current evaluated data files, TALYS and EMPIRE calculations using consistent parameter sets.

1 Introduction

Neutron-induced cross section data for Ta and W are of importance both for nuclear technologies research and development and for basic studies. The neutron-induced reaction cross sections on W isotopes and Ta have been experimentally studied around 14 MeV however due to the high threshold for most of the reactions, measurements at higher incident neutron energies are needed to guide evaluations and model calculations. Precise experimental cross section data for fast neutron-induced reactions are of considerable interest for testing nuclear model calculations. Several reaction channels are energetically allowed in the investigated energy range and different reaction mechanisms play a roll. A precise and complete experimental data base for a given mass region allows systematic development of nuclear model parameterizations.

2 Experimental procedure

The cross sections were determined by the activation method in combination with γ -spectrometry. A detailed description of the measurement technique was given elsewhere [1].

The irradiations were carried out at the 7-MV Van de Graaff accelerator at IRMM, Geel. Quasi-monoenergetic neutrons with energies between 13.8 and 20.5 MeV were produced via the $^3\text{H}(d,n)^4\text{He}$ reaction at $E_d = 1, 2, 3, 4$ MeV. The distance between the sample stack and the center of the target varied from 3 cm for samples with 10 mm diameter to 7 cm for samples with 30 mm diameter.

The neutron fluence rate was determined by the $^{27}\text{Al}(n,\alpha)^{24}\text{Na}$ ENDF/B-VI standard cross section. Due to the difference in the studied reactions half-lives the

$^{27}\text{Al}(n,p)^{27}\text{Mg}$, $^{56}\text{Fe}(n,p)^{56}\text{Mn}$, $^{58}\text{Ni}(n,p)^{58}\text{Co}$, and $^{93}\text{Nb}(n,2n)^{92\text{m}}\text{Nb}$ secondary standard were used as well.

Both isotopically enriched and natural abundance materials were employed in these measurements. Disc-shaped high-purity natural chromium ($\text{Ø}30 \times 5$ mm), nickel ($\text{Ø}14 \times 5$ mm), copper ($\text{Ø}20 \times 5$ mm), and tantalum ($\text{Ø}15 \times 1$ mm) samples were employed in the present measurements.

Table 1. Isotopic composition of enriched and natural W samples.

A	Isotopic abundance (%)				
	^{182}W	^{183}W	^{184}W	^{186}W	natW
180	<0.03	–	<0.003	<0.005	0.12(1)
182	91.6	2.11(2)	0.82	0.65	26.50(16)
183	5.03	96.30(3)	1.34	0.45	14.34(4)
184	2.46	1.58(2)	95.2	2.2	30.64(2)
186	0.91	0.005(2)	2.64	96.7	28.43(19)

Natural tungsten samples were prepared by either punching discs of 13 mm diameter or by cutting squares of 1 cm^2 from a metallic foil. Depending on the energy of the measured γ -rays samples with 0.1 or 0.25 mm thickness were used in order to minimize γ -ray attenuation. The enriched ^{182}W , ^{183}W , ^{184}W and ^{186}W samples were prepared from metal powder canned in plexiglass containers. The isotopic composition of the samples used for the cross section measurements on W isotopes is given in table 1.

The radioactivity of the samples was measured by γ -ray spectrometry. In addition to the standard detector efficiency calibration a Monte Carlo simulation of the coaxial HPGe detector was performed with the MCNP5 code in order to

achieve higher geometry flexibility and better accuracy. Both full-energy peak and total efficiencies for the detector measuring geometry were calculated with the MCNP5 code for large Cr, Ni, Cu and Ta samples as well as for W samples due to the high γ -ray attenuation. In order to increase counting statistics, a stack of several W samples were irradiated, and spread on the detector cap to avoid counting loss due to gamma-ray absorption. The decay parameters applied in the data analysis are given in table 2. The coincidence summing correction was applied in the case of the ^{48}V , ^{56}Co , ^{59}Fe , $^{178\text{m}}\text{Lu}$, $^{178\text{g}}\text{Lu}$, $^{180\text{m}}\text{Hf}$, ^{181}Hf , ^{182}Ta , ^{83}Ta , ^{184}Ta , ^{183}Hf , ^{185}Ta , ^{186}Ta , and $^{185\text{m}}\text{W}$ activities measurements. The calculated values were experimentally verified by measurement at 5.5 cm distance from the detector.

Table 2. Decay data of measured reaction products ref. [2].

Reaction	$T_{1/2}$	E_γ (keV)	I_γ (%)
$^{50}\text{Cr}(n,x)^{48}\text{V}$	15.9735(25)d	983.525	99.89(4)
$^{58}\text{Ni}(n,p\alpha)^{54}\text{Mn}$	312.12(10) d	834.848(3)	99.976(1)
$^{58}\text{Ni}(n,x)^{56}\text{Co}$	77.233(27) d	846.771	99.935(25)
$^{63}\text{Cu}(n,p\alpha)^{59}\text{Fe}$	44.495(9)	1099.245(3)	56.5(18)
		1291.590(6)	43.2(14)
$^{181}\text{Ta}(n,\alpha)^{178\text{g}}\text{Lu}$	28.4(2) min	1340.8(2)	3.42(16)
$^{181}\text{Ta}(n,\alpha)^{178\text{m}}\text{Lu}$	23.1(3) min	426.36(5)	97.0(18)
$^{181}\text{Ta}(n,x)^{180\text{m}}\text{Hf}$	5.5(1) h	332.275(11)	94.1(12)
$^{181}\text{Ta}(n,p)^{181}\text{Hf}$	42.39(6) d	482.10(9)	80.5(4)
$^{184}\text{W}(n,\alpha)^{181}\text{Hf}$			
$^{181}\text{Ta}(n,2n)^{180\text{g}}\text{Ta}$	8.154(6) h	93.4(2)	4.51(16)
$^{183}\text{W}(n,x)^{182}\text{Ta}$	114.43(4) d	1221.4	27.0(5)
$^{183}\text{W}(n,p)^{183}\text{Ta}$	5.1(1) d	246.0587(12)	27(4)
$^{184}\text{W}(n,x)^{183}\text{Ta}$			
$^{184}\text{W}(n,p)^{184}\text{Ta}$	8.7(1) h	414.01(5)	72(3)
$^{186}\text{W}(n,\alpha)^{183}\text{Hf}$	1.067(17) h	783.753(21)	66(7)
$^{186}\text{W}(n,x)^{185}\text{Ta}$	49.4(15) min	177.59(8)	25.7(4)
$^{186}\text{W}(n,p)^{186}\text{Ta}$	10.5(3) min	122.3(1)	25(4)
		737.5(3)	29(4)
$^{186}\text{W}(n,2n)^{185\text{m}}\text{W}$	1.67(3) min	131.55(2)	4.33(13)

Additional corrections applied in the data analysis were: variation of the neutron fluence during irradiation, dead time effects, low energy neutron background, neutron flux end energy distribution inside the stack of sample and monitor foils.

3 Results and discussion

The measured cross sections are shown graphically in figs. 1–6 together with experimental data measured by other authors, retrieved from the EXFOR [5], current evaluated data files [6]–[9], TALYS [4] and EMPIRE-II [3] calculations using consistent parameter sets.

The $^{50}\text{Cr}(n,x)^{48}\text{V}$, $^{58}\text{Ni}(n,p\alpha)^{54}\text{Mn}$, $^{58}\text{Ni}(n,x)^{56}\text{Co}$, $^{63}\text{Cu}(n,p\alpha)^{59}\text{Fe}$, reaction cross sections (fig. 1). Due to the generally low cross sections for (n,t) or multiple charge particle emission cross sections in the investigated energy range, care was taken for possible interference with reactions that occur on other isotopes or impurities in the

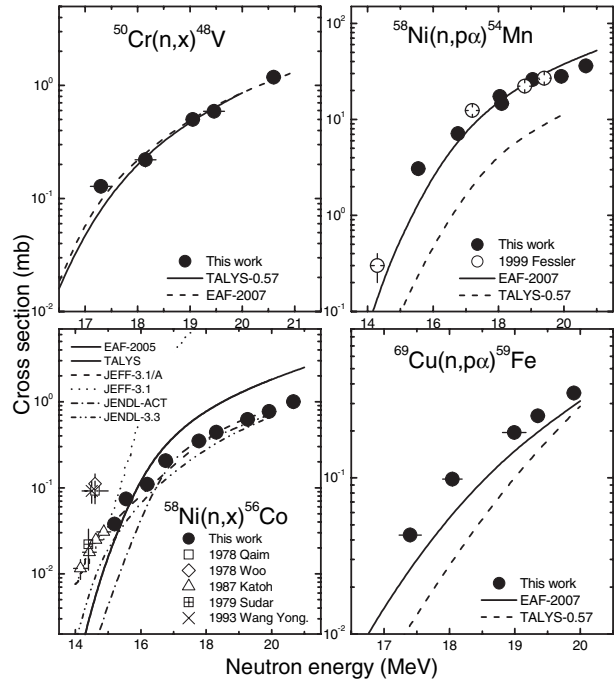


Fig. 1. Excitation functions of neutron-induced tritium and multiple charged-particle production reactions on Cr, Ni, and Cu isotopes.

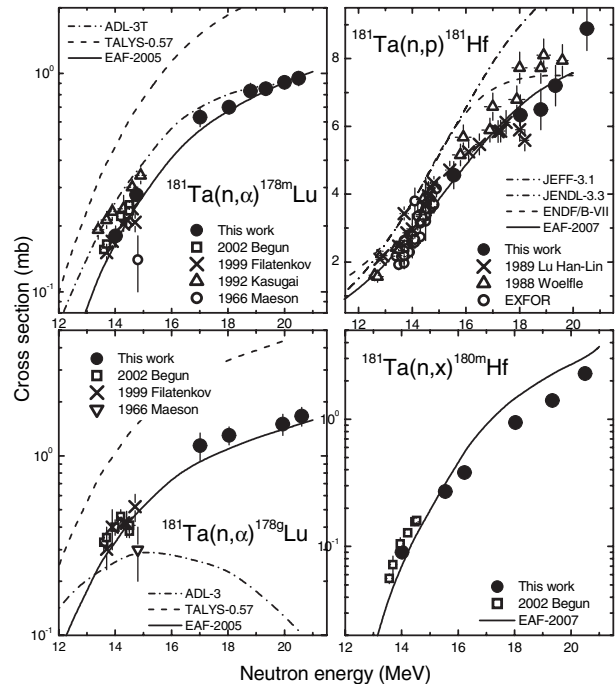


Fig. 2. Excitation functions of neutron-induced light charged-particle production reactions on Ta.

sample leading to the same product. The threshold of the reactions which contribute to the ^{48}V production from ^{50}Cr are 12.9 MeV for (n,t), 19.3 MeV for (n,nd) and 21.6 MeV for (n,2np) reactions respectively. So we can consider the $^{50}\text{Cr}(n,x)^{48}\text{V}$ reaction as a pure (n,t) reaction in the investigated energy range. Our results for the $^{50}\text{Cr}(n,x)^{48}\text{V}$ reaction are in a very good agreement with EAF-2007

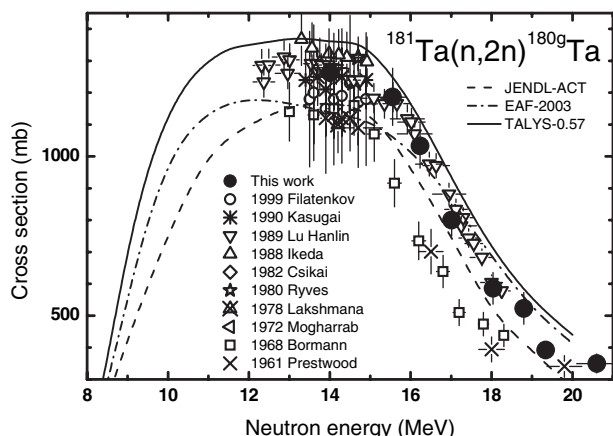


Fig. 3. Excitation functions of $^{181}\text{Ta}(n,p)^{180g}\text{Ta}$ reaction.

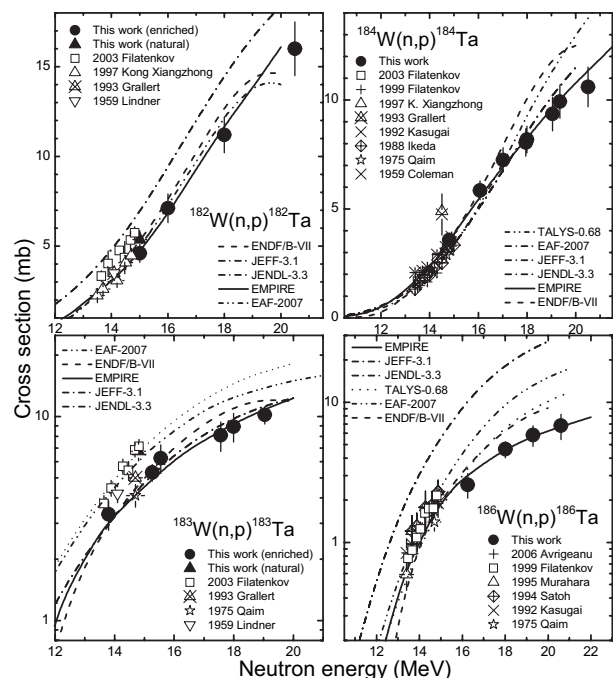


Fig. 4. Excitation functions of (n,p) reactions on W isotopes.

and TALYS-0.57 calculations. The new results for the $^{58}\text{Ni}(n,p)^{54}\text{Mn}$ reaction agree with the data of Fessler et al. and the EAF-2007 evaluation. We consider that a contribution from the $^{55}\text{Mn}(n,2n)^{54}\text{Mn}$ reaction is less than 1% based on the 100 ppm Mn impurity in the sample, given by the supplier, and the assumption that the cross section is 800 mb. The estimated contribution from the $^{54}\text{Fe}(n,p)^{54}\text{Mn}$ reaction is less than 0.1% assuming 200 mb for this reaction cross section and 40 ppm Fe impurity.

Regarding the $^{58}\text{Ni}(n,x)^{56}\text{Co}$ reaction the potential interference comes from the $^{58}\text{Ni}(n,3n)^{56}\text{Ni}$ and $^{58}\text{Ni}(n,3p)^{56}\text{Mn}$ reactions. Both reactions were discarded because the threshold of the first one is 22.9 MeV and the contribution from the second reaction will be low due to Coulomb barriers. The experimental data for the $^{58}\text{Ni}(n,x)^{56}\text{Co}$ reaction around 14 MeV split into two groups. Our results are in agreement with the

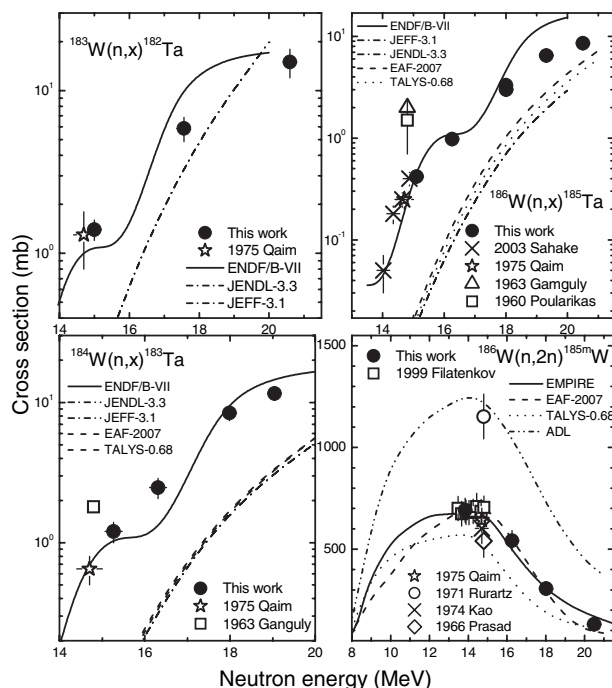


Fig. 5. Excitation functions of (n,np) reactions on W isotopes.

data of Sudar et al. and Katoh et al. Impurities of Fe, Co and Ni in the Cu sample can contribute to the production of ^{59}Fe by the $^{58}\text{Fe}(n,\gamma)^{59}\text{Fe}$, $^{59}\text{Co}(n,p)^{59}\text{Fe}$, and $^{62}\text{Ni}(n,\alpha)^{59}\text{Fe}$ reactions respectively. However there were no traces found from the activities produced by other high cross section reactions on the above mentioned elements in the measured spectra.

The neutron-induced reaction cross sections on ^{181}Ta (figs. 2 and 3). Unique data above 14 MeV were produced for the $^{181}\text{Ta}(n,x)^{180}\text{Hf}$, $^{181}\text{Ta}(n,\alpha)^{178m}\text{Lu}$, and $^{181}\text{Ta}(n,\alpha)^{178g}\text{Lu}$ reactions. Our results are in agreement with most of the data from other authors at 14 MeV for charged-particle production reaction cross sections. Good agreement was found with the EAF-2007 evaluation for all reaction cross sections. The new data tend to agree better with the data of Lu Hanlin et al. (1989) both for the $^{181}\text{Ta}(n,2n)^{180g}\text{Ta}$ and $^{181}\text{Ta}(n,p)^{181}\text{Hf}$ reaction cross sections. The 93.4 keV γ -line was used to measure $^{181}\text{Ta}(n,2n)^{180g}\text{Ta}$ reaction cross section. However ^{180m}Hf emits 93.325 keV γ -ray with 17.1% emission probability. The contribution of $^{181}\text{Ta}(n,x)^{180m}\text{Hf}$ reaction to the 93.4 keV γ -line was found to be negligible in comparison with the $^{181}\text{Ta}(n,2n)^{180g}\text{Ta}$ reaction based on the measurement of the decay curve.

The neutron-induced reaction cross sections on W isotopes (figs. 4–6). Unique data above 14 MeV were produced for all the studied reactions. Our results are in agreement with most of the data from other authors at 14 MeV for the $^{184}\text{W}(n,p)^{184}\text{Ta}$ reaction cross section. The results from this work both for $^{182}\text{W}(n,p)^{182}\text{Ta}$ and $^{183}\text{W}(n,p)^{183}\text{Ta}$ obtained with enriched samples are 20% lower than the recent Filatenkov data obtained with natural material. However contributions from the $^{183}\text{W}(n,np)$ and $^{184}\text{W}(n,np)$ reactions to the ^{182}Ta and ^{183}Ta production respectively can not be neglected even around 14 MeV. Our analysis for the $^{182}\text{W}(n,p)^{182}\text{Ta}$ and $^{183}\text{W}(n,x)^{182}\text{Ta}$ reaction cross sections

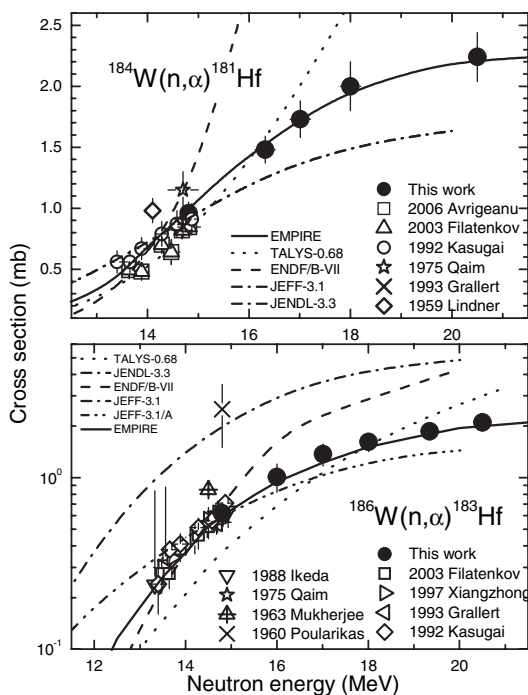


Fig. 6. Excitation functions of (n,α) reactions on W isotopes.

are based on 1221.4 keV gamma-line, which is less intensive than 1121.3 keV to avoid interference with the natural background for the former one. Our preliminary data for the $^{186}\text{W}(n,p)^{186}\text{Ta}$ reaction cross section seem to be 10 to 15% lower than the others around 14 MeV, however measurement of the decay curve of the 197.9 keV gamma-line (the most intensive from ^{186}Ta) used for most of the results around 14 MeV showed possible interference as well.

Very few data for the (n,np) reaction cross sections on W isotopes exist in EXFOR. In all cases our results are in good agreement with the results of Qaim et al. from 1975 and the results of Sahake et al. from 2003 for the $^{186}\text{W}(n,x)^{185}\text{Ta}$ reaction cross sections. An enriched in ^{186}W sample was used for the $^{186}\text{W}(n,2n)^{185m}\text{W}$ reaction cross section measurements due to the interference from $^{184}\text{W}(n,\gamma)^{185m}\text{W}$ induced from the low-energy neutrons. Our results agree with the data of Filatenkov et al. at 14 MeV and with the EAF-2007 evaluation.

Concerning the $^{184}\text{W}(n,\alpha)^{181}\text{Hf}$ and the $^{186}\text{W}(n,\alpha)^{183}\text{Hf}$ reaction cross sections the experimental data around 14 MeV are relatively consistent, however the differences in the evaluated nuclear data files from the major data libraries are considerable. Our results for both reactions are in a good

agreement with the data around 14 MeV and the EMPIRE model calculations.

4 Summary and conclusions

Cross sections for $^{50}\text{Cr}(n,x)^{48}\text{V}$, $^{58}\text{Ni}(n,p\alpha)^{54}\text{Mn}$, $^{58}\text{Ni}(n,x)^{56}\text{Co}$, $^{63}\text{Cu}(n,p\alpha)^{59}\text{Fe}$, $^{181}\text{Ta}(n,\alpha)^{178m}\text{Lu}$, $^{181}\text{Ta}(n,\alpha)^{178g}\text{Lu}$, $^{181}\text{Ta}(n,x)^{180m}\text{Hf}$, $^{181}\text{Ta}(n,p)^{181}\text{Hf}$, $^{181}\text{Ta}(n,2n)^{180g}\text{Ta}$, $^{182}\text{W}(n,p)^{182}\text{Ta}$, $^{183}\text{W}(n,x)^{182}\text{Ta}$, $^{183}\text{W}(n,p)^{183}\text{Ta}$, $^{184}\text{W}(n,x)^{183}\text{Ta}$, $^{184}\text{W}(n,\alpha)^{181}\text{Hf}$, $^{184}\text{W}(n,p)^{184}\text{Ta}$, $^{186}\text{W}(n,\alpha)^{183}\text{Hf}$, $^{186}\text{W}(n,x)^{185}\text{Ta}$, $^{186}\text{W}(n,p)^{186}\text{Ta}$, and $^{186}\text{W}(n,2n)^{185m}\text{W}$ reactions were measured by the activation technique in the energy range from 13.5 to 20.6 MeV relative to $^{27}\text{Al}(n,\alpha)^{24}\text{Na}$ standard reaction cross section. The use of enriched samples allowed distinguishing activity produced by different reactions leading to the same product. The new experimental data improve the knowledge of the excitation functions of the investigated reactions substantially and two of the reactions were measured for the first time. The data were shown to be essential for the model calculations.

The authors are grateful to the IRMM Van de Graaff Laboratory personnel for providing us with the best possible experimental conditions.

References

1. V. Semkova, A. Avrigeanu, T. Glodariu, A.J. Koning, A.J.M. Plompen, D.L. Smith, S. Sudár, Nucl. Phys. A **730**, 225 (2004).
2. Nuclear Data Sheets, <http://www.nndc.bnl.gov/nndc/ensdf/>, <http://www.nea.fr>, <http://www-nds.iaea.org/ensdf/>.
3. R. Capote (these proceedings).
4. A.J. Koning, S. Hilaire, M.C. Duijvestijn, in *Proceedings of the International Conference on Nuclear Data for Science and Technology, ND2004, Sept. 26–Oct. 1, 2004, Santa Fe, USA*, edited by R. Haight, M. Chadwick, T. Kawano, P. Talou. (AIP, Melville, New York, 2005), p. 1154.
5. EXFOR, <http://www-nds.iaea.org/exfor/>.
6. M.B. Chadwick, P. Oblozinsky et al., Nucl. Data Sheets **107**(12), 2931 (2006).
7. JEFF-3.1, JENDL-3.3, <http://www.nndc.bnl.gov/nndc/ensdf/>, <http://www.nea.fr>, <http://www-nds.iaea.org/ensdf/>.
8. EAF-2007, <http://fusion.org.uk/easy2007>.
9. ADL-3, <http://t2.lanl.gov/data/ndviewer.html>.